Low Temperature Volatile-Organic-Compound (VOC) Sensor Based on Tungsten Oxide Nanorods

Yong Shin Kim[*], Youn Tae Kim[*], and Kwangyeol Lee[**]

[*]Electronics and Telecommunications Research Institute (ETRI), 161 Gajong-dong, Yusong-gu, Daejeon 305-350, Republic of Korea, yongshin@etri.re.kr and ytkim@etri.re.kr
[**] Department of Chemistry, Korea University, Seoul 136-701, Republic of Korea, kylee1@korea.ac.kr

ABSTRACT

Tungsten oxide sensors were fabricated by using highly crystalline and homogeneous $WO_{2.72}$ nanorods with average 75-nm length and 4-nm diameter. They provide unique opportunities for investigating the effects of size-controlled tungsten oxide nanorods on vapor detection. Here, we report excellent sensing ability of the nanorod sensors at low operation temperature, even ambient temperature, upon exposure to volatile organic compounds (VOCs).

Keywords: gas sensor, tungsten oxide, metal oxide semiconductor, VOC sensor, $WO_{2.72}$ nanorod

1 INTRODUCTION

Metal-oxide-semiconductor (MOS) gas sensors are very promising devices due to their high sensitivity, small dimensions, low cost, and good compatibility with the fabrication process for microelectronic devices. They generally operate at high temperature of 200 – 500°C on the basis of the modification of electrical conductivity of MOS active layers, resulting from the interactions between ionosorbed oxygen moieties (O_2^-, O^- and O^{-2} species) and gas molecules to be detected. In conventional MOS sensors consisting of polycrystalline metal oxide particles, only the species adsorbed near grain boundaries are operative in modifying the electrical transport properties and therefore the gas-sensing ability has been hampered by low surface-to-volume ratio.

One-dimensional (1-D) nanostructures with high surface-to-volume ratio and small grain size have attracted much current attention as candidate materials for MOS gas sensors. Recently, individual nanomaterials such as carbon nanotube, SnO_2 and In_2O_3 nanowires had successfully applied to the gas sensor devices [1-3]. They exhibited novel properties such as high sensitivity, fast response time, and room temperature operation, which are unattainable by the conventional MOS materials. The major drawback, however, remains due to difficulties in mass production of sensors based on individual 1-D nanostructures.

Nanosized tungsten oxide particles have been found useful in fabricating gas sensors for the detection of nitrogen oxides, ammonia, and hydrogen sulfide. Current research, however, has focused on the use of polycrystalline tungsten oxide systems and thus important sensor requirements such as high sensitivity and low temperature operation have not been accomplished. We have recently reported a single step, large scale preparation of single-crystalline, size-controlled tungsten oxide nanorods [4], thus providing a singular research opportunity for tungsten oxide-based gas sensor development.

Here, we report to prepare porous tungsten oxide films made of highly-crystalline, phase-pure nanorod materials, and to present their excellent gas-sensing properties at low temperature. These films could be easily fabricated by wet processes and their sensing characteristics were found to be superior to those of conventional MOS. In addition, the compatibility of wet processes with microelectronic fabrication offers particular opportunities for development of inexpensive sensor systems in the cost-conscious gas sensor market.

2 FABRICATION OF $WO_{2.72}$ SENSORS

2.1 Preparation of Sensor Substrate

We used two kinds of sensor substrates: one had detection electrodes on glass for room temperature operation and another was microheater-embedded membrane one fabricated by Si-bulk micromachining, as previously reported in detail [5], for high temperature operation with minimized power consumption. Figure 1 shows a cross-sectional schematic diagram of the Si sensor device. The well structure with the membrane was fabricated by the anisotropic wet etching of bulk Si using 5 wt.% tetra-methyl ammonium hydroxide (TMAH) solution. The interdigitated detection electrodes have 100-μm width and 300-μm spacing. The heater line (25-μm width and spacing) simultaneously acts as a temperature-measuring resistor.
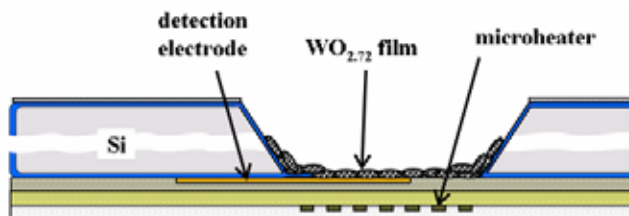

Figure 1: Cross-sectional schematic structure of our tungsten oxide nanorod sensor.

2.2 Formation of WO$_{2.72}$ Nanorod Films

Tungsten oxide (WO$_{2.72}$) nanorods with 4-nm diameter and aspect ratio of ~20 were synthesized according to our colloid-based synthetic approach [4]. As-synthesized solution was treated by adding diluted HCl solution and resulting WO$_{2.72}$ precipitation was then separated by a centrifuge in order to remove the amine-based surfactant. The product was further purified by dissolving in toluene and sequential centrifuging three times. The isopropyl alcohol solution of tungsten oxide nanorods prepared by ultrasonic treatment was dispensed onto the detection electrodes, and then was dried at 100°C under vacuum for 10 h. In addition, WO$_{2.72}$ films on Si were also prepared for material analysis under the same conditions.

2.3 Evaluation of Gas-Sensing Properties

Gas-sensing measurements were carried out by placing a gas sensor in a small detection chamber with electrical feedthroughs, and by blowing analyte vapors over it with the flow rate of 1000 ml/min. The analyte concentration was regulated with the relative flow ratio between carrier air and diluted analyte vapor in the flow injection measurement system. The diluted sample was prepared with a fixed concentration in a gas cylinder or by regulating the vapor pressure of liquid analyte with the variation of the temperature of its containing reservoir. The detection performance and characteristics were performed upon exposure of several volatile organic compounds (VOCs) such as methanol, benzene, acetone and toluene.

For measuring the change of sensor resistance upon analyte exposure, sensor interface circuitry was made on printed circuit board. It consists of voltage divider and amplification circuits. The measured analog signals are delivered to the digital interface (NI, DAQ 6062E) connected to laptop PC through a shielded cable. The data acquisition was performed by the user software programmed under LabVIEW (NI) environments with the sampling rate of 10 Hz.

3 RESULTS AND DISCUSSION

3.1 Material Analyses on WO$_{2.72}$ Films

Figure 2 shows the typical surface morphology of resultant tungsten oxide film, observed by scanning electron microscope (SEM). It displays porous appearance resulting from the randomly arranged linear aggregates formed by parallel alignment of individual WO$_{2.72}$ nanorods. The high porosity has advantages from the viewpoint of the response time of a gas sensor due to the high diffusion rate of analyte molecules into the sensing layer.
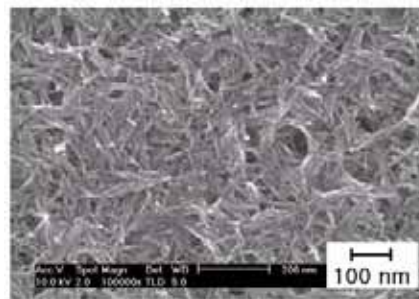

Figure 2: Surface SEM image of WO$_{2.72}$ nanorod film.

XRD patterns displayed the (010) peak of monoclinic WO$_{2.72}$ [W$_{18}$O$_{49}$], assigned to the growth direction of the rods [4], together with broad background peaks due to the small nanorod dimension. Furthermore, the Raman shift bands observed at 264, 325, 709, and 805 cm^{-1} give additional evidence to the monoclinic structure (see Fig. 3). There is additional sharp peak positioned at 514nm because of the excitation source of Ar-ion laser.
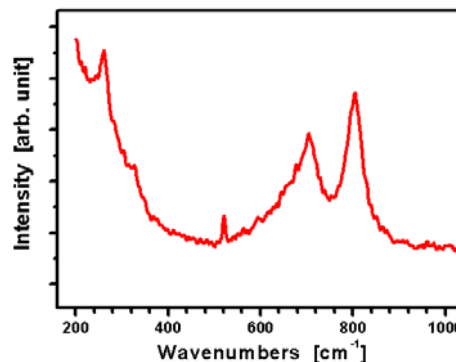

Figure 3: Raman spectrum of WO$_{2.72}$ nanorod film.

In order to evaluate the constituents of the WO$_{2.72}$ films, XPS analysis was also performed. The wide scan XPS spectrum shown in Fig. 4 demonstrates that they compose predominantly of tungsten and oxygen atoms together with only small amount of carbon impurities, which could be easily introduced from carbon dioxide at atmosphere or from solvents and reactants at the synthesis step.
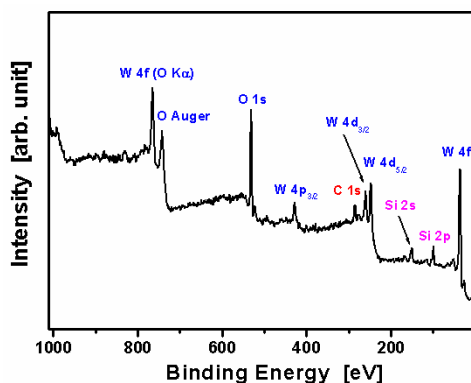

Figure 4: Wide scan XPS spectrum of WO$_{2.72}$ film.

Consequently, the tungsten oxide nanorod film used as a sensing element can be considered simply as the condensed collectivity of randomly arranged bundles of monoclinic $WO_{2.72}$ nanorods (75-nm length and 4-nm diameter) with high porosity and only little carbon impurities.

3.2   Gas-Sensing Properties of $WO_{2.72}$ Devices

Detailed experiments were performed for ethanol exposure to elucidate the gas-sensing characteristics of our $WO_{2.72}$ nanorod sensors, carefully. Figure 5 shows the typical response profiles as a function of measurement time with increasing an ethanol concentration from 4.1 to 130 ppm at room temperature. The inset plot displays the relationship between the ethanol concentration and the response magnitude, the relative sensor resistance variation to the initial one. It shows the empirical relationship of *response = A × [concentration]$^\beta$*, where *A* is the prefactor and β the exponent. The response time is found to be larger than 20 min at room temperature. However, it become shorter as the operation temperature goes higher. Previously, we observed the response time for ammonia detection to be less than 2 min at operation temperature of 70°C [6].
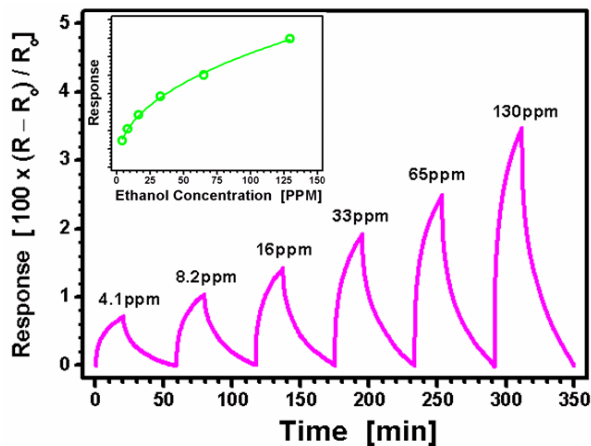

Figure 5: Concentration dependence of the sensor response for ethanol exposure at room temperature.

The ambient measurements were found to be accelerated by heating the sensing materials around 100°C for short duration less than 1 min or by illuminating UV light. Figure 6 shows the prompt recovery of sensor resistance into the initial value by 365-nm UV exposure for 10 seconds. It can be understood with the increase in desorption rate of adsorbed analytes by the imparted thermal or photon energy. Similar behaviors at room temperature were previously reported in the SnO_2 nanoribbon gas sensor system [7]. These phenomena are important for achieving a practical MOS gas sensor operated under ambient conditions with a reasonable recovery time.
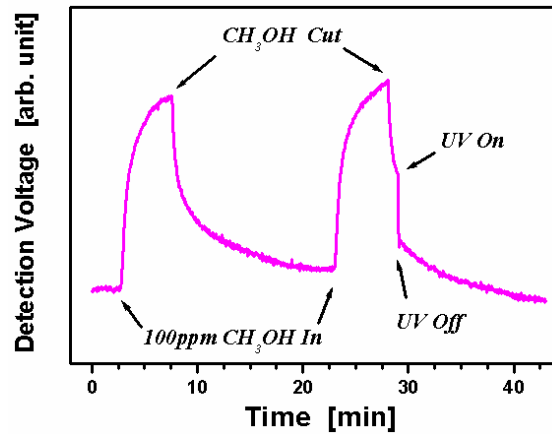

Figure 6: UV light effect on the recovery time

Figure 7 shows the response time profiles of three $WO_{2.72}$ films with the different thicknesses of 1.2, 4.6, and 7.0 μm. They display nearly identical response shape, which implies that the response and recovery times are independent on the sensing layer thickness. In conventional MOS sensor, the response time becomes longer as the film thickness goes higher because of the difference in the diffusion time of analyte molecules into the sensing layer. Therefore, the identical response irrespective of the film thickness could be explained with the high porosity of our $WO_{2.72}$ films as observed in the SEM image.
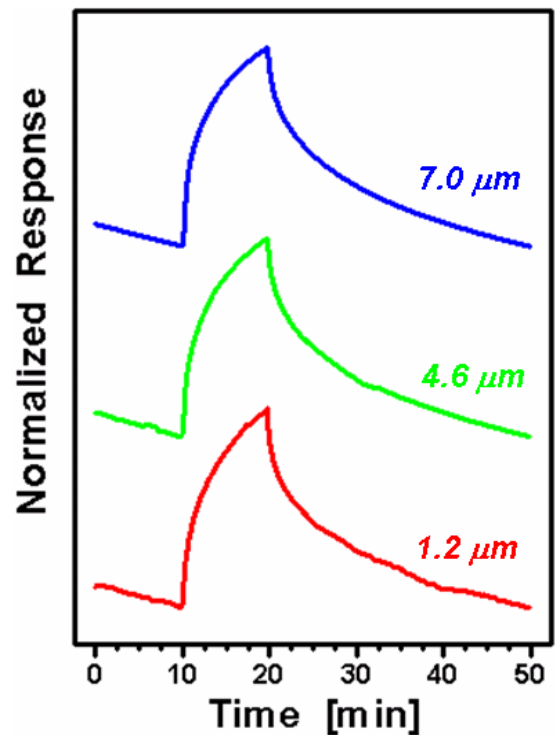

Figure 7: Ethanol response profiles for $WO_{2.72}$ sensing layers with different thickness.
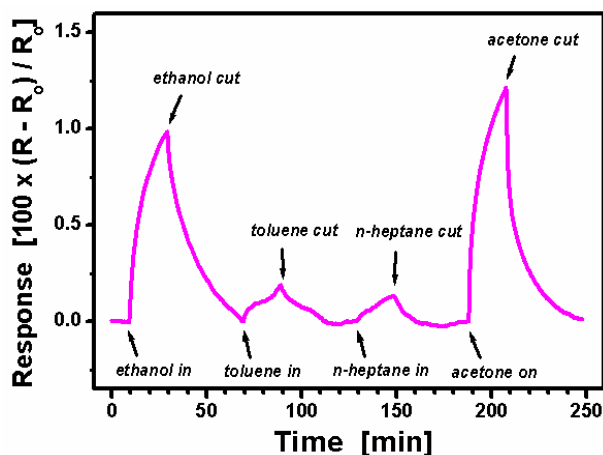
Figure 8: Various volatile organic compounds detection of tungsten oxide nanorod sensor at room temperature.

Figure 8 shows the detection response of our sensor at room temperature for low-concentration VOC exposures: ethanol, toluene, *n*-heptane, and acetone vapors with the concentration of about 3 ppm. It clearly demonstrates the high detection sensitivity for various VOCs at ambient temperature. Our previous study had shown the sensitive detection of reducing ammonia gas in addition to oxidizing nitrogen dioxide [6]. In addition, there was found to be some possibility for obtaining the selectivity among analyte vapors by means of the temperature-dependent response variation.

4   CONCLUSION

We have fabricated tungsten oxide nanorod sensors by using highly crystalline, tiny $WO_{2.72}$ nanorods. They show gas-sensing capability for various VOCs with about 3-ppm concentration, even at room temperature. The recovery time can be shortened by short heating pulse or UV illumination. These excellent sensing properties seem to be attributed to the unique structural features of $WO_{2.72}$ nanorod-based films with a high surface-to-volume ratio and highly adsorption-active sites due to the nonstoichiometric nature. The facile VOC detection at ambient temperatures suggests that tungsten oxide nanorod sensors might be successfully employed for the miniaturized sensing system, fulfilling the requirement of low power consumption.

ACKOWLEGEMENT

REFERENCES

[1] J. Kong, N. R. Franklin, C. Zhou, M. G. Chapline, S. Peng, K. Cho, and H. Dai, Science 287, 622, 2000.
[2] A. Kolmakov, Y. Zhang, G. Cheng, and M. Moskovits, Adv. Mater. 15, 997, 2003.
[3] C. Li, D. Zhang, X. Liu, S. Han, T. Tang, J. Han, and C. Zhou, App. Phys. Lett. 82, 1613, 2003.
[4] K. Lee, W. S. Seo, and J. T. Park, J. Am. Chem. Soc. 125, 3408, 2003.
[5] S.-C. Ha, Y. S. Kim, Y. Yang, Y. J. Kim, S.-M. Cho, H. Yang, and Y. T. Kim, Sen. Actuators B in press.
[6] Y. S. Kim, S.-C. Ha, K. Kim, H. Yang, S.-Y. Choi, Y. T. Kim, J. T. Park, C. H. Lee, J. Choi, J. Paek and K. Lee, Appl. Phys. Lett. in submitted.
[7] M. Law, H. Kind, B. Messer, F. Kim, and P. Yang, Angew. Chem. Int. Ed. 41, 2405, 2002.